Fast Data Sorting with Modified Principal Component Analysis to Distinguish Unique Single Molecular Break Junction Trajectories

J. M. Hamill,[1,*] X. T. Zhao,[2] G. Mészáros,[3] M. R. Bryce,[2] and M. Arenz[1]
[1]Department of Chemistry and Biochemistry, University of Bern, Freiestrasse 3, CH-3012 Bern, Switzerland
[2]Department of Chemistry, Durham University, Durham DH1 3LE, United Kingdom
[3]Research Centre for Natural Sciences, Hungarian Academy of Sciences, Magyar Tudósok Körútja 2, H-1117 Budapest, Hungary

(Received 21 June 2017; published 2 January 2018)

A simple and fast analysis method to sort large data sets into groups with shared distinguishing characteristics is described and applied to single molecular break junction conductance versus electrode displacement data. The method, based on principal component analysis, successfully sorts data sets based on the projection of the data onto the first or second principal component of the correlation matrix without the need to assert any specific hypothesis about the expected features within the data. This is an improvement on the current correlation matrix analysis approach because it sorts data automatically, making it more objective and less time consuming, and our method is applicable to a wide range of multivariate data sets. Here the method is demonstrated on two systems. First, it is demonstrated on mixtures of two molecules with identical anchor groups and similar lengths, but either a π (high conductance) or a σ (low conductance) bridge. The mixed data are automatically sorted into two groups containing one molecule or the other. Second, it is demonstrated on break junction data measured with the π bridged molecule alone. Again, the method distinguishes between two groups. These groups are tentatively assigned to different geometries of the molecule in the junction.

DOI: 10.1103/PhysRevLett.120.016601

Extremely large data sets, especially as a result of automated measurements, are becoming more common. Quick and powerful methods are required to sift through the data and organize it to save room on hard drives, save time in analysis, and focus on significant results. This must be done in unbiased ways. Here, single molecular break junction (SMBJ) conductance traces were measured, and a new statistical analysis method was used to sort the data into groups with unique characteristics. We first demonstrate that this method separates the distinctive junctions of one molecule or the other when two molecules are mixed in solution. We then demonstrate that the same method sorts junctions with a single molecule alone into separate groups of junctions. This allows for a more comprehensive analysis of the experimental results.

Automated SMBJ experiments result in terabytes of traces with a broad sampling of gold-molecule-gold junctions, including the following types: (1) junctions which do not break cleanly due to contamination or environmental disruptions, (2) junctions which break cleanly but contain no molecule, (3) junctions which break cleanly and contain multiple molecules, and (4) junctions that break cleanly and contain a single molecule. Usually only junctions of type 4 are interesting for further analysis. Preanalysis methods are often employed to filter the data, with varying degrees of objectivity. Recently, new methods [1–3] have analyzed large SMBJ data sets without making *a priori* assumptions about molecular plateau shape, and without resorting to hand sorting and subjective filtering choices.

Type 4 junction trajectories have a wide degree of variability due to a number of stochastic processes involved [4,5]. Calculations predict correlations between junction geometries and molecular conductance [6]. However, conductance changes between different junction geometries are often indistinguishable.

The method developed by Halbritter *et al.* [7] distinguishes important junction trajectories. The method calculates 1D histograms from each conductance versus displacement trace and compiles them into a data matrix, $\mathbf{X}$, with m rows of histogram bins and n separate measurements. The correlation matrix, C, for $\mathbf{X}$ is calculated by

$$C_{i,j} = \frac{\langle [x_i - \langle x_i \rangle][x_j - \langle x_j \rangle] \rangle}{\sqrt{\langle [x_i - \langle x_i \rangle]^2 \rangle \langle [x_j - \langle x_j \rangle]^2 \rangle}}, \tag{1}$$

where x_i and x_j represent histogram counts in bins i and j, and $\langle x_i \rangle$ represents the average value of variable x_i over all traces. The numerator in Eq. (1) calculates the average covariance between conductance bins i and j. The denominator scales the numerator so that the values of C range from $[-1, 1]$. When $C_{i,j} = 0$, there is no correlation between conductance bins i and j. When $C_{i,j} > 0$ ($C_{i,j} < 0$), there is a correlation (anticorrelation) between conductances corresponding to bins i and j. Generally, conductance bins i and j are correlated when there is a probability of plateaus

occurring in traces at both conductances together in the same trace. Anticorrelation may indicate that there is a probability that if a plateau occurs at conductance bin i, then there will be no plateau at conductance bin j. The next step in this method requires making certain assumptions about the trajectories of the break junctions, and then separating the data into groups based on those assumptions. Our new approach does not require these assumptions, saving time and increasing objectivity.

The established method of principal component analysis (PCA) [8–11] provides a statistically rigorous, objective tool for sorting data sets. PCA is a common method applied in a variety of disciplines including neural networks [12], chemometrics [11], and geospatial statistics [13].

A summary of the relevant mathematics behind PCA can be found in the Supplemental Material [14]. In short, diagonalizing C [Eq. (1)] and sorting the eigenvectors in decreasing size of eigenvalues yields an orthogonal basis set, with the first eigenvector PC_1 describing the direction of the most variance in the data set, and the second eigenvector PC_2 describing that of the second most variance, etc. There are many software packages which implement PCA by adapting this fundamental mathematical concept for use in specific fields. For instance, Unscrambler X [15] and PLS Toolbox [16] are two implementations focused on spectroscopy. Here we demonstrate our own adaptation.

An intuitive understanding of PCA can be obtained by reducing the problem to a ball on a spring oscillating in three dimensions [Fig. 1(a)]. Although the ball is oscillating in a particular direction due to the large influence of the spring, there will be smaller influences in other directions. C will be a 3×3 matrix describing how the three variables correlate with one another. Diagonalizing C will result in three eigenvalue-eigenvector pairs. The eigenvector corresponding to the largest eigenvalue, PC_{sp}, will point along the direction of the oscillating spring. The other eigenvectors, PC_a and PC_b, will point orthogonal to the spring oscillations, in directions corresponding to smaller influences.

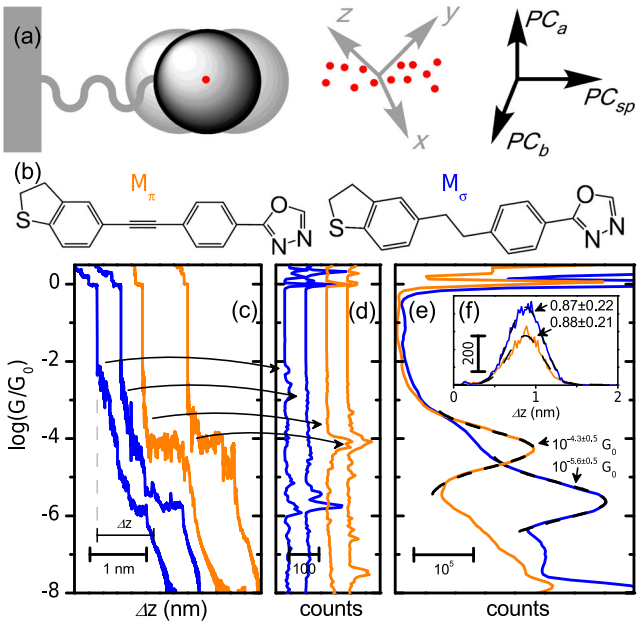

FIG. 1. (a) PCA demonstration schematic. (b) Break junction results for $\mathbf{M}_\pi$ (orange) and $\mathbf{M}_\sigma$ (blue). (c) Example conductance traces. (d) Example conductance traces binned into single 1D histograms. (e) Total 1D histograms accumulated from 86% of 8801 ($\mathbf{M}_\pi$) and 96% of 12 033 traces ($\mathbf{M}_\sigma$)—molecular peaks fit to Gaussian (curves). (f) Plateau length histograms calculated as the displacement of each trace between $10^{-0.3}G_0$ and $10^{-6.5}G_0$.

This basic understanding applies to the following analysis. To sort traces, the procedure will be to project all measurements onto one PC and sort them depending on whether they project positively or negatively. In the above analogy, this is equivalent to sorting the measurements into groups based on whether they are on the elongated part of the spring motion or the compressed part. See the Supplemental Material [14] (which includes Refs. [17–19]), where we demonstrate that when the number of measurements is larger than about 1000, PCA is computationally faster than another recent method [2] introduced to categorize SMBJ traces.

To test the ability for PCs to effectively sort SMBJ data sets into single-mode distributions, two molecules, $\mathbf{M}_\pi$ and $\mathbf{M}_\sigma$ [Fig. 1(b)], were synthesized with identical anchoring groups and similar lengths, but different conductances due to the π or σ bridge (see the Supplemental Material [14], which includes Ref. [20], for synthesis details). The molecules were chosen so that a mixture of the molecules can be measured using SMBJs (see the Supplemental Material [14] for SMBJ experimental details), and both will anchor identically and compete equally for the break junction. The molecules were also chosen because there was no expected specific interaction between $\mathbf{M}_\pi$ and $\mathbf{M}_\sigma$ when mixed in solution.

First, $\mathbf{M}_\pi$ and $\mathbf{M}_\sigma$ were measured separately with SMBJ. Traces [Fig. 1(c)] showed a difference in conductance in the molecular plateau between $\mathbf{M}_\pi$ and $\mathbf{M}_\sigma$. The conductance traces were then binned into 1D histograms [Fig. 1(d)]. The data matrices, $\mathbf{X}_\pi$ and $\mathbf{X}_\sigma$, had single 1D histograms as columns, and histogram bins as rows. The sum of each row produced total 1D histograms [Fig. 1(e)]. $\mathbf{X}_\pi$ and $\mathbf{X}_\sigma$ were easily distinguishable by the difference in location of the molecular conductance peak, with $10^{-4.3}G_0$ for $\mathbf{M}_\pi$ and $10^{-5.6}G_0$ for $\mathbf{M}_\sigma$, as determined by fitting the peaks to a Gaussian. Although the molecular conductances changed by over 1 order of magnitude, the plateau lengths, accumulated into plateau length histograms [Fig. 1(f)], showed no difference in the average plateau length between $\mathbf{M}_\pi$ and $\mathbf{M}_\sigma$.

Next, a 1:3 (No./No.) mixture of $\mathbf{M}_\pi$ and $\mathbf{M}_\sigma$ (**Mix 1**) was measured (see the Supplemental Material [14] for results for two other mixtures). Due to the differences in conductance between $\mathbf{M}_\pi$ and $\mathbf{M}_\sigma$, we anticipated a bimodal distribution. To test our method, we needed to show that PC sorting can distinguish the two contributing classes of events. 1D histograms were created from each trace [Fig. 2(a)], and these were accumulated into a data

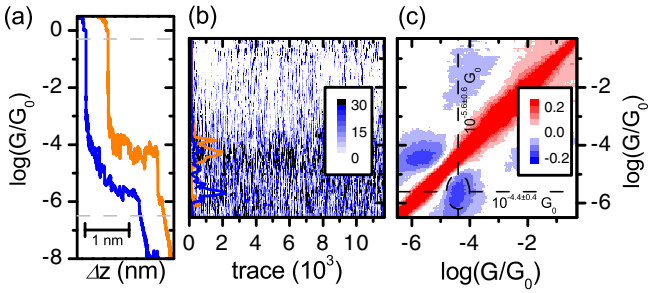

FIG. 2. Break junction results for **Mix 1**. (a) Example traces with corresponding 1D conductance histograms in (b). (b) Data matrix of $n = 11671$ traces binned into single histograms. (c) 2D correlation histogram calculated from data matrix.

matrix [Fig. 2(b)]. The bins corresponding to the gold-gold junction and open circuit were removed [gray dashed lines in Fig. 2(a)], and the correlation matrix was calculated. An intensity plot of the correlation matrix was plotted [Fig. 2(c)]. Figure 2(c) had a region of anticorrelation at $(10^{-4.3}G_0, 10^{-5.6}G_0)$, which suggested that the traces in the data set had a plateau at the molecular conductance of $\mathbf{M}_\pi$ or $\mathbf{M}_\sigma$, but not both.

Following the guidelines outlined in Ref. [21], the next steps in analyzing **Mix 1** would require formulating a hypothesis about the expected shape of the conductance traces that yielded the anticorrelation region, and then sorting the traces into groups using these conditions. The method proposed in this Letter forgoes these assumptions.

Instead, the correlation matrix was diagonalized and the eigenvalues were sorted in decreasing order. The corresponding eigenvectors were sorted with the eigenvalues.

The questions of which eigenvectors to use in further analysis, and how many, are poorly resolved [11]. A variety of criteria are suggested with the caveat that, regardless of method, one must test and check based on the results. For our study, it was necessary to find the minimum number of PCs with the highest variance explained that distinguished between two different conductance features. We found that either PC_1 or PC_2 [Fig. 3(a)] was sufficient to do this. More PCs may contain other details about the data set, but these details were not the focus of this study. To determine which, PC_1 or PC_2, to use in the final steps of the sorting, two criteria were used: (1) a score plot, PC_1 vs PC_2 [Fig. 3(b)], aided in understanding the relative importance of PC_1 and PC_2 with respect to each other; and (2) the PC had to work. Criterion 1 aided in objectively choosing the appropriate PC, because we were predominantly concerned with a PC which found the largest distinctions between traces with features associated either with $\mathbf{M}_\pi$ or with $\mathbf{M}_\sigma$. When the bin coefficients in Fig. 3(b) for either PC_1 or PC_2 were close to zero, then those bins did not contribute to that PC. On the other hand, when the bin coefficients for a PC were large, either positively or negatively, then those bins were significant. Thus, large coefficients in the region of the molecular conductance and small coefficients elsewhere in

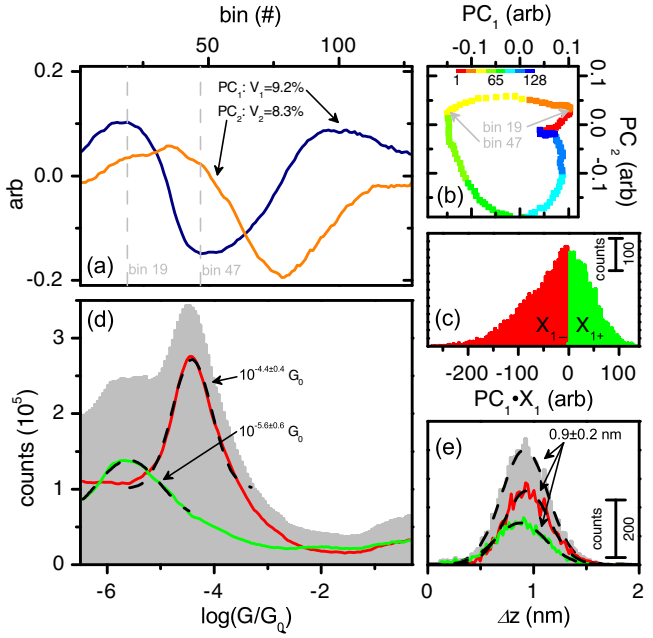

FIG. 3. Principal component sorting on **Mix 1** using PC_1. (a) PC_1 (blue) and PC_2 (orange) plotted vs bin number. (b) PC_1 vs PC_2 from bin 1 (red) to bin 128 (blue). (c) Histogram constructed from single 1D histograms projected onto PC_1—curves in the red (green) bins had negative (positive) projections. (d) Negatively (7129 curves) and positively (4541 curves) projected curves sorted into separate groups and total (80% of 14 543 curves) 1D histograms (gray). (e) Plateau lengths were determined for each trace in the negative (red) and positive (green) subgroups, and the entire data set (gray), and histograms were constructed for each.

the PC were desirable. But since the toolbox of PCA does not provide a definitive test to choose PCs, criterion 2 was also necessary. Criterion 2 had the potential to be a subjective criterion, but it was very clear when the PC successfully sorted the molecules and when it did not, and in every case either PC_1 or PC_2 did this effectively. When the PC successfully sorted the traces, the total 1D histograms for each group were single-mode Gaussian distributions with little or no shoulders. When the PC did not successfully sort the traces, the 1D histograms retained a bimodal distribution or large shoulders. If neither PC_1 nor PC_2 fulfilled either criterion 1 or criterion 2, it would be necessary to move on to other PCs. PCs after PC_2 (see Fig. S9 in the Supplemental Material [14] for the first eight PCs) followed a qualitatively different pattern from PCs 1 and 2. The variances explained declined rapidly, suggesting that the first PCs were more significant than the others (see the Supplemental Material [14]).

For the example of **Mix 1**, bins 19 and 47 were the bins where PC_1 was maximum and minimum, and closely corresponded to bins with conductances of $\mathbf{M}_\sigma$ and $\mathbf{M}_\pi$, respectively, so PC_1 was chosen to complete the analysis. In this case, PC_2 would not sort molecules because it was maximum at $10^{-2}G_0$, and this was in a region outside the

range of the molecular conductances. This region showed up in Fig. 2(c) as the weak anticorrelation region at $(10^{-2}G_0, 10^{-4}G_0)$ (see the Supplemental Material [14] for PC sorting using PC_2). PC_1 accounted for over 9% of the variance of the entire data set, while the remaining 127 eigenvectors together accounted for the remaining 91%. Studying PC_1 alone retained much of the important variability of the data, while significantly reducing the complexity of the analysis by focusing on one dimension. If more PCs were used to create a multidimensional feature vector, it was possible to overfit the results. For the current Letter, we chose the smallest number of PCs that still yielded reasonable results, and a single PC was sufficient to do this. It was remarkable that 9% variance explained was sufficient to distinguish between different conductance features in our data. For other systems—for instance, systems with larger signal-to-noise ratios—larger variance explained may be appropriate.

Next, each 1D histogram was projected onto PC_1, and the 1D histograms were separated into positive and negative groups, $\mathbf{X}_{1+}$ (4541 curves) and $\mathbf{X}_{1-}$ (7129 curves), respectively, based on the sign $(+/-)$ of the dot product [Fig. 3(c)]. Each group was separately summed into total 1D histograms [Fig. 3(d)] and compared to Fig. 1(d). Our method successfully separated the histograms into high-conductance ($\mathbf{X}_{1-}$) and low-conductance groups ($\mathbf{X}_{1+}$), corresponding to junctions involving $\mathbf{M}_\pi$ and $\mathbf{M}_\sigma$, respectively. Finally, the length histograms for the sorted groups were compared to the length histograms for the entire set [Fig. 3(e)]. The average plateau lengths for each group were the same, and matched both the average plateau length of the entire set, and the average plateau lengths when the molecules were measured separately [Fig. 1(e)].

As proof of concept, the results above showed the ability of PC sorting to distinguish obvious bimodal features in data sets with a change in conductance of over 1 order of magnitude between $\mathbf{M}_\pi$ and $\mathbf{M}_\sigma$. Next, we showed that PC sorting can perform a very useful task: it can distinguish groups with a change in conductance of about half an order of magnitude and an associated change in plateau length of about 0.15 nm. Changes in conductance like this are common in optically [22] and electrochemically [23] switched SMBJs. Furthermore, 0.15 nm represents the radius of a gold atom and the bottom limit of measurable differences between groups.

The SMBJ results for $\mathbf{M}_\pi$ were analyzed using the same procedures outlined above. PC_2 was used to separate the single histograms into positive ($\mathbf{X}_{\pi-}$) and negative ($\mathbf{X}_{\pi+}$) groups (Fig. 4; see the Supplemental Material [14] for PC sorting steps). $\mathbf{X}_{\pi+}$ had a larger molecular conductance in the 1D histogram [Fig. 4(a)] and a longer plateau length [Fig. 4(c)] compared to $\mathbf{X}_{\pi-}$. Most traces in $\mathbf{X}_{\pi+}$ had long, flat plateaus resulting in a narrow total 1D histogram. The average master curves were calculated to visualize an average trace (see the Supplemental Material [14] for

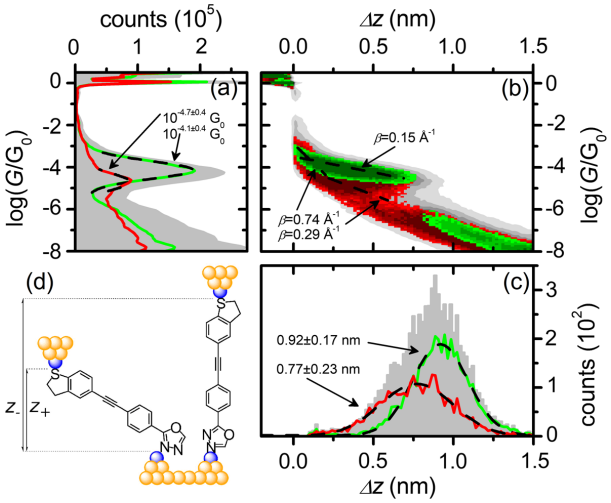

FIG. 4. PC sorting of the $\mathbf{M}_\pi$ data set (86% of 8801 curves) into positive ($\mathbf{X}_{\pi+}$, green, 3151 curves) and negative ($\mathbf{X}_{\pi-}$, red, 4419 curves) subgroups using PC_2. (a) Total 1D histograms with Gaussian fits. (b) 2D histograms with master curve linear fit of plateaus. (c) Plateau length histograms with Gaussian fits. (d) Cartoon depicting possible junction geometry leading to $\mathbf{X}_{\pi-}$ and $\mathbf{X}_{\pi+}$.

details) [24]. The slope β of the plateau region in the master curve for $\mathbf{X}_{\pi+}$ was determined to be 0.15 Å^{-1} with a linear fit. Traces in $\mathbf{X}_{\pi-}$ were less homogeneous, with fewer long and flat plateaus and a broader distribution of steeper slopes. The slope of the master curve in the plateau region of group $\mathbf{X}_{\pi-}$ was also drastically different: the master curve had two regions in the molecular plateau with two separate slopes, 0.74 and 0.29 Å^{-1}. The slope of the plateau of a SMBJ trace was shown to be proportional to the tunneling decay constant of the gold-molecule-gold system [25]. The gold-molecule-gold system can be modeled as a square potential barrier yielding an exponential dependence of tunneling conductance with length:

$$G = A \exp(-\beta l), \tag{2}$$

where A captures parameters in the contacts and l is the width of the potential well [26]. Thus, the doubling of the tunneling decay constant between $\mathbf{X}_{\pi+}$ and $\mathbf{X}_{\pi-}$ reflected an important change in the tunneling behavior of $\mathbf{M}_\pi$. An average slope of 0.15 Å^{-1} for $\mathbf{X}_{\pi+}$ matched other conjugated molecules, which were shown to have slopes of 0.1–0.4 Å^{-1}. Likewise, an average slope of 0.74 Å^{-1} for $\mathbf{X}_{\pi-}$ matched saturated molecules, which were shown to have slopes of 0.6–1.0 Å^{-1} [25].

Because the sorting process was objective and statistically relevant, we were encouraged to speculate about the physical differences leading to the sorted groups. If the sorting was a result of decisions about expected trace shapes, assertions about the physical interpretations of the data will likely reinforce the subjective decisions applied. Instead, PC sorting allows the experimentalist to make

confident hypotheses which can better inform new directions of investigation, including simulations to test the hypotheses.

With this in mind, we attempt here to interpret the results of the PC sorting on $\mathbf{M}_\pi$. PC_2 had the second largest variance explained of the 128 eigenvectors of $\mathbf{X}_\pi$, accounting for 8% of the variance. We hypothesized $\mathbf{X}_{\pi+}$ comprised mostly of junctions in which the end groups of $\mathbf{M}_\pi$ bonded strongly and bridged the electrodes in a nearly perpendicular geometry. This geometry yielded a high conductance, low tunneling decay constant, and long plateau length. We further hypothesized $\mathbf{X}_{\pi-}$, comprised of junctions in which the 1,3,4-oxadiazole end group of $\mathbf{M}_\pi$ was more weakly bonded to one electrode, most likely slipped along the electrode (thus achieving at least two metastable geometries responsible for two distinct tunneling decay regions), and never achieved a full chemisorbed bond with the electrode, which would have resulted in identical conductance and length as $\mathbf{X}_{\pi+}$. It was shown [6] that a bonding geometry in which the conductance pathway does not align with the Au electrode will yield a lower conductance.

The PC sorting method described in this Letter provides a means to sort a large data set into groups based on statistically distinctive characteristics, allowing the groups to be studied separately, and it allows two particular groups to be compared meaningfully to theoretical predictions based on models of ideal junctions. No *a priori* hypothesis needs to be imposed regarding expected conductance trace shape. In this Letter, the PCs were treated separately, yielding an intrinsically 1D analysis by comparing either/or behavior of the data set. Presented here was a technique which can be applied to many data sets across many disciplines. Many variables can be included in a data matrix, including measurements from conducting force spectroscopy and optical measurements. Also, multiple PCs may be treated as a single feature vector—the result would be a PC sorting based on higher-dimensional, more complex criteria.

The authors are grateful to Dr. Wenjing Hong for molecule designs. J. M. H. is grateful to James Bevington and Veerabhadrarao Kaliginedi for illuminating discussions. This work was generously supported by EC FP7 ITN "MOLESCO" Project No. 606728, and by the University of Bern.

*joseph.hamill@gmail.com

[1] A. Magyarkuti, K. Lauritzen, Z. Balogh, A. Nyáry, G. Mészáros, P. Makk, G. Solomon, and A. Halbritter, J. Chem. Phys. **146**, 092319 (2017).
[2] M. Lemmer, M. S. Inkpen, K. Kornysheva, N. J. Long, and T. Albrecht, Nat. Commun. **7**, 12922 (2016).
[3] M. S. Inkpen, M. Lemmer, N. Fitzpatrick, D. Costa-Milan, R. J. Nichols, N. J. Long, and T. Albrecht, J. Am. Chem. Soc. **137**, 9971 (2015).
[4] S. Guo, J. Hihath, I. Díez-Pérez, and N. Tao, J. Am. Chem. Soc. **133**, 19189 (2011).
[5] J. A. Malen, P. Doak, K. Baheti, T. D. Tilley, A. Majumdar, and R. A. Segalman, Nano Lett. **9**, 3406 (2009).
[6] M. Kamenetska, M. Koentopp, A. C. Whalley, Y. S. Park, M. L. Steigerwald, C. Nuckolls, M. S. Hybertsen, and L. Venkataraman, Phys. Rev. Lett. **102**, 126803 (2009).
[7] A. Halbritter, P. Makk, S. Mackowiak, S. Csonka, M. Wawrzyniak, and J. Martinek, Phys. Rev. Lett. **105**, 266805 (2010).
[8] K. Pearson, Lond. Edinb. Dubl. Phil. Mag. **2**, 559 (1901).
[9] I. Jolliffe, *Principal Component Analysis* (Wiley Online Library, New York, 2002).
[10] J. Shlens, arXiv:1404.1100.
[11] R. Bro and A. K. Smilde, Anal. Methods **6**, 2812 (2014).
[12] J. Karhunen and J. Joutsensalo, Neural Netw. **7**, 113 (1994).
[13] J. Bevington, D. Piragnolo, P. Teatini, G. Vellidis, and F. Morari, Geoderma **262**, 294 (2016).
[14] See Supplemental Material at http://link.aps.org/supplemental/10.1103/PhysRevLett.120.016601 for synthesis and experimental details and a brief summary of the mathematics behind principal component analysis.
[15] H. Martens, T. Karstang, and T. Ns, J. Chemom. **1**, 201 (1987).
[16] B. M. Wise and N. B. Gallagher, Eigenvector Technol. **196** (1998).
[17] T. Elgamal and M. Hefeeda, arXiv:1503.05214v2.
[18] J. Gan and Y. Tao, in *Proceedings of the 2015 ACM SIGMOD International Conference on Management of Data* (ACM, New York, USA, 2015), pp. 519–530.
[19] J. W. Eaton, D. Bateman, S. Hauberg, and R. Wehbring, *GNU Octave Version 3.8.1 Manual: A High-Level Interactive Language for Numerical Computations* (Network Theory Limited, Bristol, UK, 2014), http://www.gnu.org/software/octave/doc/interpreter/.
[20] N. Salvanna, G. C. Reddy, B. R. Rao, and B. Das, RSC Adv. **3**, 20538 (2013).
[21] P. Makk, D. Tomaszewski, J. Martinek, Z. Balogh, S. Csonka, M. Wawrzyniak, M. Frei, L. Venkataraman, and A. Halbritter, ACS Nano **6**, 3411 (2012).
[22] B. E. Tebikachew, H. B. Li, A. Pirrotta, K. Börjesson, G. C. Solomon, J. Hihath, and K. Moth-Poulsen, J. Phys. Chem. C **121**, 7094 (2017).
[23] A. C. Aragonès, D. Aravena, F. J. Valverde-Muñoz, J. A. Real, F. Sanz, I. Díez-Pérez, and E. Ruiz, J. Am. Chem. Soc. **139**, 5768 (2017).
[24] P. Moreno-García, M. Gulcur, D. Z. Manrique, T. Pope, W. Hong, V. Kaliginedi, C. Huang, A. S. Batsanov, M. R. Bryce, C. Lambert, and T. Wandlowski, J. Am. Chem. Soc. **135**, 12228 (2013).
[25] C. Huang, A. V. Rudnev, W. Hong, and T. Wandlowski, Chem. Soc. Rev. **44**, 889 (2015).
[26] J. G. Simmons, J. Appl. Phys. **34**, 1793 (1963).